JACS
JOURNAL OF THE AMERICAN CHEMICAL SOCIETY

Article

pubs.acs.org/JACS

A Carbohydrate-Derived Splice Modulator

Sachin Dhar,[†] James J. La Clair,*[,†] Brian León,[†] Justin C. Hammons,[†] Zhe Yu,[‡] Manoj K. Kashyap,[‡] Januario E. Castro,[‡] and Michael D. Burkart*[,†]

[†]Department of Chemistry and Biochemistry, University of California−San Diego, 9500 Gilman Drive, La Jolla, California 92093-0358, United States

[‡]Moores Cancer Center, University of California−San Diego, La Jolla, California 92093-0358, United States

Supporting Information

ABSTRACT: Small-molecule splice modulators have recently been recognized for their clinical potential for diverse cancers. This, combined with their use as tools to study the importance of splice-regulated events and their association with disease, continues to fuel the discovery of new splice modulators. One of the key challenges found in the current class of materials arises from their instability, where rapid metabolic degradation can lead to off-target responses. We now describe the preparation of bench-stable splice modulators by adapting carbohydrate motifs as a central scaffold to provide rapid access to potent splice modulators.

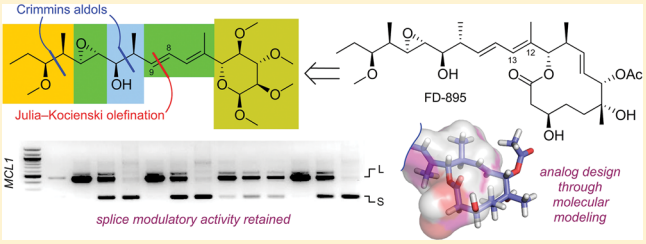

INTRODUCTION

In 2007, two Japanese teams revealed the importance of targeting the SF3b unit of the spliceosome for antitumor therapy.[1,2] These breakthroughs not only forwarded the spliceosome as an important target for cancer[2] but also identified two key families of polyketide spliceosome modulators (Figure 1), including FD-895 (**1a**),[2] pladienolide B (**1b**),[3] and herboxidiene (**1c**).[4] Since these discoveries, the development of splicing assays has been instrumental in the advance of next generation splice modulators. The success of these discoveries was further marked by the translation of an analog of pladienolide D, E7101, into phase I clinical trials.[5] However, many of these natural products are subject to low stability and/or poor pharmacological properties.[6] To this end, our laboratory has been part of a growing medicinal chemistry effort to identify next generation splice modulators with improved pharmacological properties.

An attractive proposal developed by Webb suggested a method of analog development through the use of a consensus motif.[7] Pursuing this approach, their team has advanced the sudemycins[8] and a pladienolide−herboxidiene hybrid[9] as next-generation leads. This, along with efforts at the Eisai Co., Ltd.,[10] H3 Biomedicine,[11] Pfizer,[12] Ghosh-Jurica laboratories,[13] Koide laboratory,[14] and our laboratories,[15] have provided a strong foundation for achieving analogs with improved pharmacological properties. We now report on an advanced new class of splice modulators that are more potent, stable, and rapidly accessible analogs.

In addition to carbohydrates being ubiquitous biological scaffolds, they are also derived from the natural chiral pool, making them ideal scaffolds for medicinal chemical optimization.[16] To expand on this hypothesis, we designed and prepared carbohydrate-derived **2**, an analog of FD-895 whose core was derived from D-glucose.

RESULTS

Our design began with FD-895 (**1a**) because of the fact that earlier medicinal chemistry efforts in our laboratory provided derivatives with improved pharmacological properties.[6a] From these studies, we determined that manipulation of the stereochemistry at the C16−C17 diad (blue shaded, Figure 1) provided an effective means to improve activity. From this data, we targeted a side chain that contained the exact terminus (orange shading, Figure 1), epoxide (green shading, Figure 1), and diene groups (green shading, Figure 1) as one of our more active analogs of FD-895.[6a] Here, we incorporated already known SAR data to improve activity by selecting an improved C16−C17 stereodiad (blue shading in **2**, Figure 1).

Clues Obtained from the Solution Structure Analysis of FD-895 (1a). Although structural information on the eukaryotic spliceosome has recently been published,[18] representation of the binding of a splice modulator with SF3b has yet to be established. We began by exploring the solution structure of the macrolide core of FD-895 (**1a**). Using multiple solvents ($CDCl_3$ and C_6D_6) for data acquisition, we identified a series of NOE interactions that along with coupling constant data allowed assignment of the solution structure of the macrolide core (Figure 2a).

Design of a Carbohydrate Core Motif. Using this structure and analyzing its space-filling model, we began to search for motifs that accurately represented the macrolide core. Our goal was to find a structural unit that offered an improved

Received: December 23, 2015
Published: April 8, 2016

DOI: 10.1021/jacs.5b13427
J. Am. Chem. Soc. 2016, 138, 5063−5068

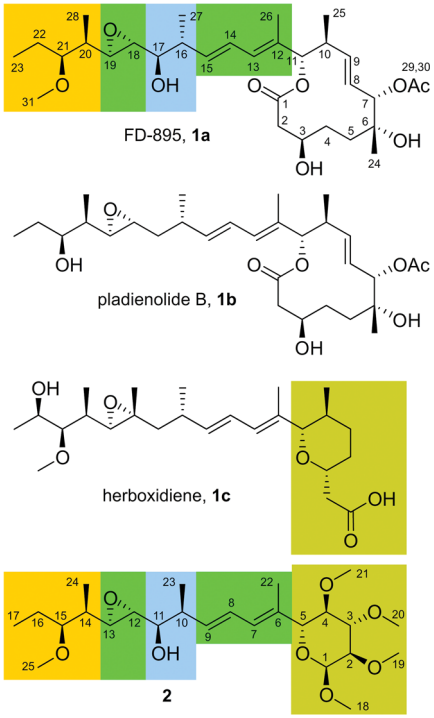

Figure 1. Structures of FD-895 (**1a**), pladienolide B (**1b**), herboxidiene (**1c**), and carbohydrate-derived splicing modulator **2**. Compound **2** contains the terminus (orange) of **1a**, the epoxide and diene of **1a** (green), and a core derived from **1c** (gold).

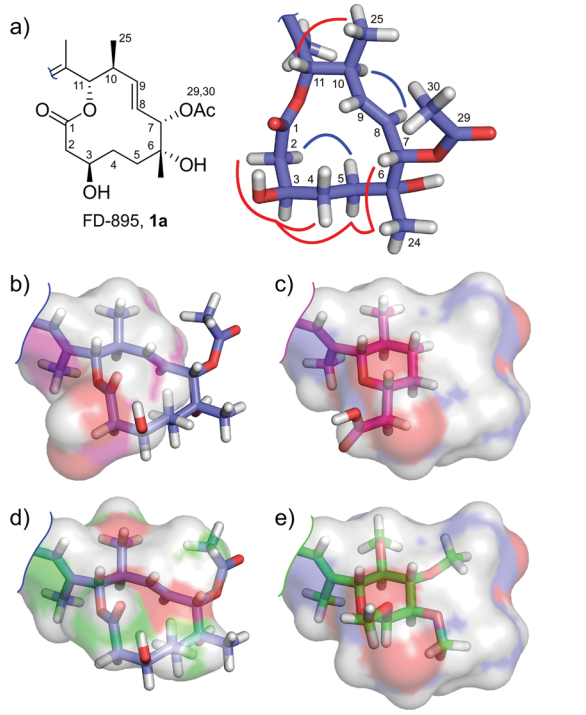

Figure 2. Models of FD-895 (**1a**, blue), herboxidiene (**1c**, magenta), and carbohydrate-derived analog **2** (green). (a) Derived solution structure of the FD-895 core motif as determined by evaluation of ^{1}H coupling constants and NOE interactions. NOE interactions were observed both on the top face (red) and bottom face (blue). Data shown was collected from $^{1}H,^{1}H$ NOESY spectral data of **1a** in $CDCl_3$ and C_6D_6 at 23 °C. (b) Model depicting the structure of **1a** (blue) superimposed on the surface of **1c** (magenta). (c) Model depicting the structure of **1c** (magenta) superimposed on the surface of **1a** (blue). (d) Models depicting the structure of **1a** (blue) superimposed on the surface of **2** (green). (e) Model depicting the structure of **2** (green) superimposed on the surface of **1a** (blue). The structure of the core motif in **1a** was determined via NMR spectroscopy. Structures of **1b** and **1c** were modeled by energy minimization.[17]

synthesis entry and diverse means of tailoring while also addressing previous pharmacological issues (stability and solubility). We began by inspecting the overlap between the small herboxidiene (**1c**) and large FD-895 (**1a**) cores. Although a clear overlay existed (Figure 1b,c), it was evident that space occupied by the C4−C7 unit within **1a** may not be a requirement for activity. We soon realized that simple monosaccharides such as D-glucose could provide a strong overlap with these cores. After evaluating several structures, we turned our attention to explore α-methyl-2,3,4-trimethoxy-D-glucopyranoside (**3**) as a core mimetic.[19]

Structurally, glycoside **2** offered a functional map that lay between the core sizes of **1a** and **1c** (Figure 2). As illustrated in Figure 2d,e, the C2−C4 methoxy groups in **2** provided a fit approximating **1a** relative to that of herboxidiene (Figure 2b,c). Specifically, the C2 methoxy group of **2** filled the space taken by the C24 methyl group in **1a**. Likewise, the C3 methoxy of **2** was able to partially fill the space of the C29−C30 acetate, a region that was already shown to tolerate functional modifications.[20] With this support, we turned our attention to synthesize and biologically evaluate analog **2**.

Synthetic Strategy. Our plan focused on using a late-stage Julia−Kocienski olefination to couple a side chain derived from FD-895 to the monosaccharide core (see Abstract graphic). Here, we envisioned that we could leverage the extensive efforts from our own laboratory for development of pladienolide/FD-895 side chain[6a,15b] as a means to probe the structure−activity relationships (SARs) of side-chain-incorporating analogs. We therefore set out toward preparation of core component **8** (Scheme 1) and side-chain component **16** (Scheme 2).

Synthesis of a Carbohydrate Core Component 8. Synthesis of **8** was accomplished in five steps from **3**, a monosaccharide derivative that in turn was prepared in three

Scheme 1. Synthesis of Core Component 8

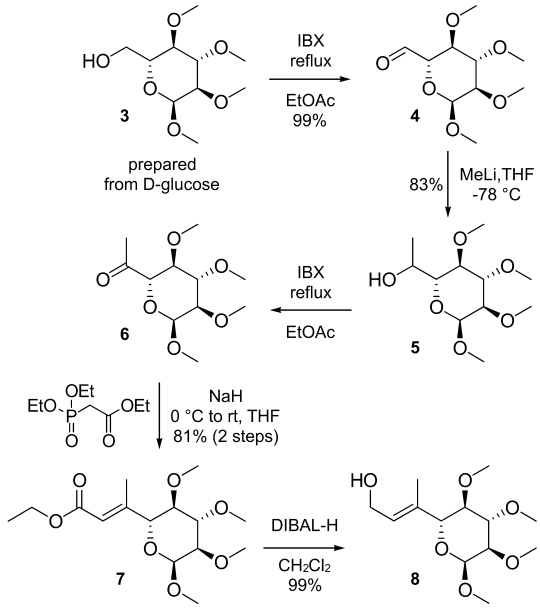

DOI: 10.1021/jacs.5b13427
J. Am. Chem. Soc. 2016, 138, 5063−5068

Scheme 2. Synthesis of Side Chain Component 16

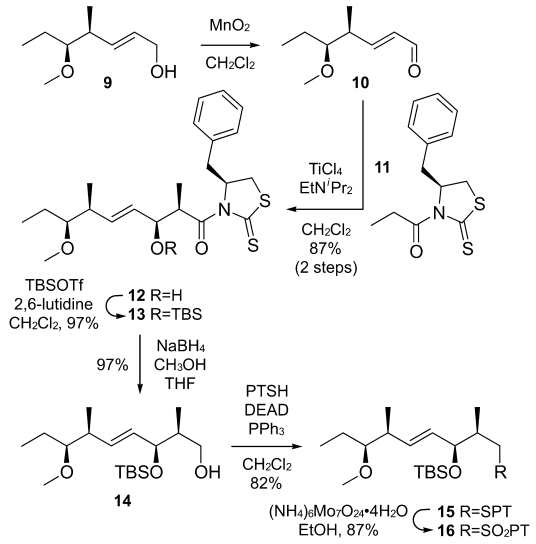

steps (54% yield) from α-methyl-D-glucopyranoside.[19] We began by oxidizing to aldehyde **4**. Advantageously, we were able to reduce chromatographic purification efforts by using a combination of an IBX oxidation followed by solvent-dependent filtration through a pad of SiO_2. The addition of MeLi to crude **4** occurred with minimal byproduct formation, providing alcohol **5** in 82% yield from **3**.

Repetition of the IBX oxidation procedure provided ketone **6**, which could be rapidly purified by passage through a SiO_2 plug. Although small samples of **6** were purified for characterization, the crude product was readily subjected to a Horner–Wadsworth–Emmons olefination to afford ester **7**. We were able to convert **5** to **7** in two steps and 80% yield with a single purification. Finally, ester **7** was reduced with DIBAL-H to afford core unit **8**, which could be stored for months at −20 °C without decomposition. Overall, this process provides access to **8** in 66% in five steps from **3** (36% in 8 steps from α-methyl-D-glucopyranoside).

Synthesis of the Side Chain Component 16. The synthesis of the side chain component began with allylic alcohol **9**, an intermediate that was prepared at >10 g scale for the synthesis of FD-895 (**1a**).[6a] Allylic oxidation with MnO_2 provided aldehyde **10**, which was purified through a SiO_2 plug and directly submitted to a Crimmins aldol reaction with auxiliary **11**, to afford adduct **12** in 87% yield over two steps. NMR analyses on the crude product indicated that this reaction occurred without detectable formation of other isomeric products.

With **12** in hand, the carbinol was protected as TBS ether **13**, and the auxiliary was removed by $NaBH_4$ reduction. Optimization studies indicated that a 5:1 ratio of THF:CH_3OH provided a reproducibly high yield of **14**. Completion of this component was accomplished by a two-step installation of the 1-phenyl-1*H*-tetrazol-5-yl (PT) sulfone. Although Mitsunobu conditions were effective at producing sulfone **15** in 82% yield at a gram scale, oxidation often provided significant quantities of the corresponding sulfoxides (incomplete oxidation byproducts). Typically, samples of these sulfoxides were collected after chromatographic purification and resubmitted to the oxidation conditions to afford a combined yield of 89% of component **16**. To date, we have completed the synthesis of gram quantities of **16** in 6 steps and 58% overall yield from **9** and 12 steps and 21% overall yield from auxiliary **11**.[6a]

Component Assembly and Completion of the Synthesis of 2. With components **8** and **16** in hand, the component coupling began by oxidizing allylic alcohol **8** to the corresponding aldehyde **17**. Purification via dry column vacuum chromatography using Geduran 60 silica gel was sufficient to afford pure **17** for coupling. After initial screening, we found the optimum yield (68%) of **18** was obtained when applying 1.05 equiv NaHMDS to 1.0 equiv of sulfone **8** and following this by addition of 1.1 equiv of aldehyde **17**. The yield of this reaction also included recovery of 8% of sulfone **16** and 11% of the chromatographically separable cis isomer of **18** (structure not shown). With samples of pure **18** on hand, deprotection with TBAF afforded alcohol **19** (Scheme 3).

Scheme 3. Component Assembly

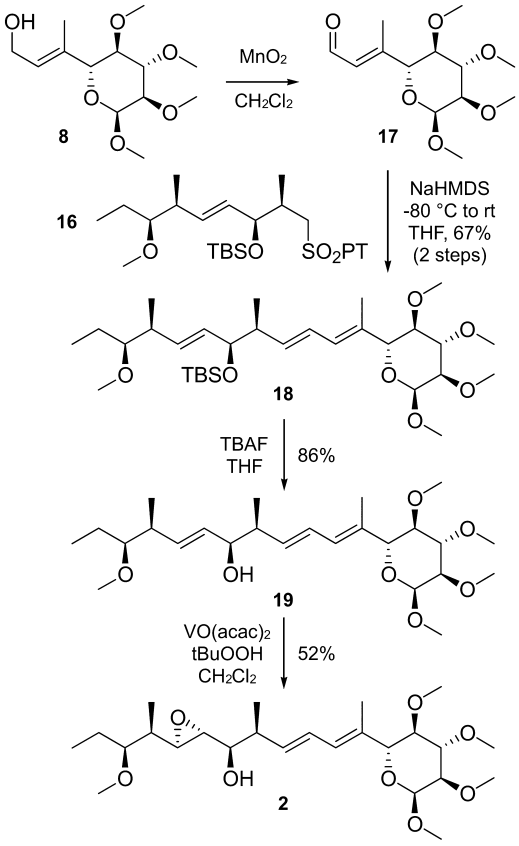

Next, we turned to the stereoselective $VO(acac)_2$-catalyzed epoxidation of allylic alcohols[21] to install the C12–C13 epoxide. As shown in Figure 3a, treatment of **19** with 4.5 equiv of tBuOOH and 3 equiv of $VO(acac)_2$ at −20 °C for 6 h provided the desired stereoisomer with ∼4:1 diastereoselectivity. Although this was the major product, over-warming or not starting the reaction at −78 °C resulted in epoxidation at C8–C9. This product was not as stable because the C11 carbinol was capable of attacking the C8 center of the epoxide, forming the corresponding furan analog (structure not shown). Although additional optimization efforts will be required, the current conditions returned **2** in 52% yield with only traces of the undesired C8–C9 epoxidation (5–10% yield).

Validation of the Structural Assignment of 2. Although the mechanism of the $VO(acac)_2$/tBuOOH epoxidation

DOI: 10.1021/jacs.5b13427
J. Am. Chem. Soc. 2016, 138, 5063–5068

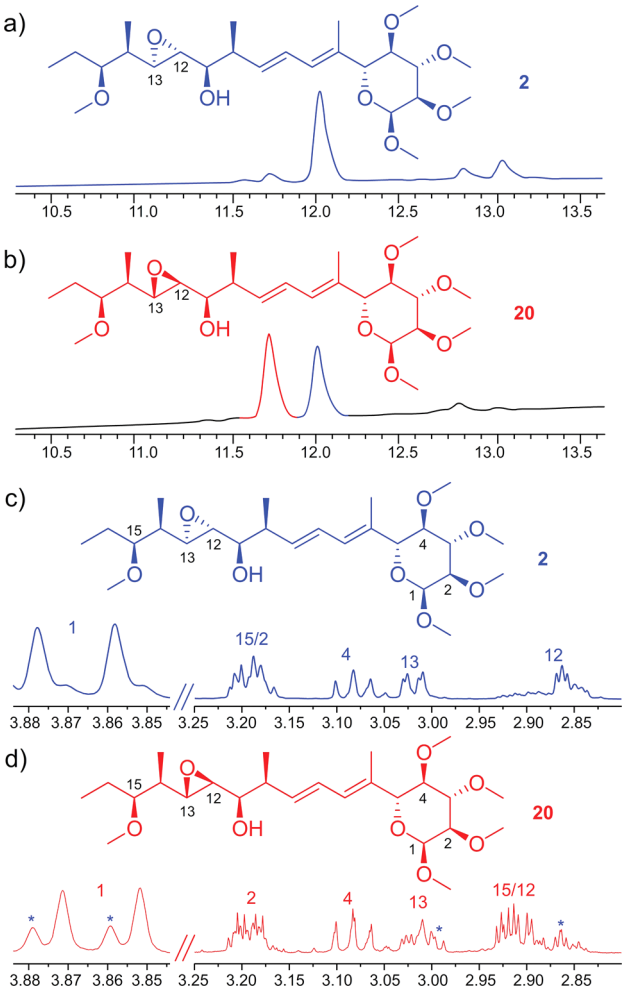

Figure 3. Stereoselectivity of the C12−C13 epoxidation. (a) Expanded LC-MS trace via UV monitoring at 288 nm depicting the reaction product from treatment of **19** with $VO(acac)_2$/tBuOOH (blue). (b) Comparable LC-MS trace depicting the formation of two isomers by *m*-CBPA epoxidation (red). (c) Expansion of the ^1H NMR spectra of epoxide **2** from $VO(acac)_2$/tBuOOH in $CDCl_3$ (blue). (d) Expansion of the ^1H NMR spectra of epoxide **20** in $CDCl_3$ from m-CBPA (red). Traces of **2** denoted by a blue asterisk could not be completely removed from **20** because of close retention times.

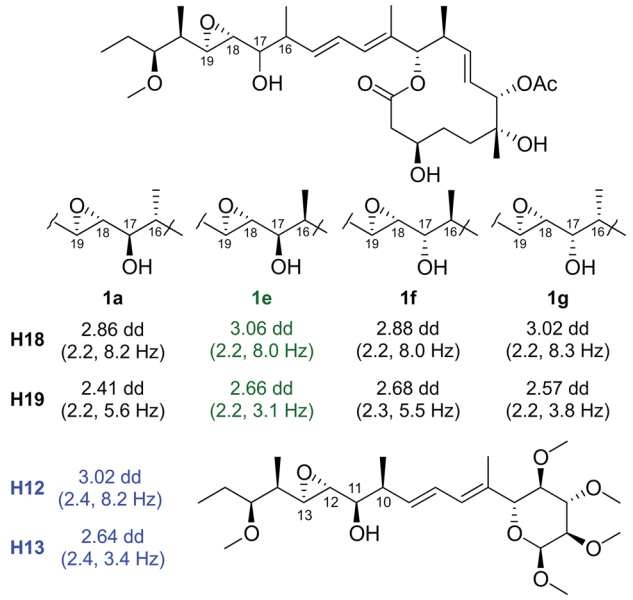

Figure 4. Coupling constant analyses. NMR analysis in C_6D_6 provided a coupling pattern at C12−C13 in **2** (blue) that matched that from the corresponding FD-895 analog **1e** (green) but not analogs **1a**, **1f**, or **1g** (black).[6a,15b]

suggests delivery of the correct stereochemical outcome, we wanted to gain further confirmation that the product was indeed **2**. We began by exploring other epoxidation conditions to prepare samples of the alternate isomer. Treatment of **19** with 1.2 equiv of *m*-CPBA at −78 °C in $NaHCO_3$-buffered CH_2Cl_2 followed by slow warming to room temperature afforded a ∼1:1 mixture of both epoxides (Figure 3b) in 62% yield. After chromatographic purification, we were able to obtain samples of both isomers.

Comparative NMR analyses on the epoxides from $VO(acac)_2$/tBuOOH and *m*-CPBA provided a solution (Figure 3c). Using 2D NMR data set (Supporting Information), we were able to fully assign the proton assignments in this product. We identified that the chemical shift and coupling patterns of the epoxide protons at C12−C13 provided the closest match to the configuration of corresponding C16−C17 isomer **1e** (Figure 4), with comparable chemical shifts and coupling constants.

Stability and Solubility of 2. Early studies indicated that **2** was more soluble and stable in aqueous buffers than FD-895 (**1a**). Using capillary NMR and solvent ^{13}C satellites (QSCS) as a means of quantitation,[22] we found that **2** was soluble up to 95 ± 5 mM D_2O/DMSO-d_6 (10:1) at 23 °C, whereas FD-895 (**1a**) was limited to 15 ± 5 mM under the same conditions. Additionally, we used NMR monitoring to show that although **1a** had a half-life of ∼70 h in D_2O/DMSO-d_6 (10:1) at 37 °C,[6a] carbohydrate analog **2** showed no signs of decomposition even after 744 h (1 month) under the same conditions. Although detailed partitioning, permeability, and metabolic stability analyses are ongoing, this initial evidence suggests that **2** offers the potential to improve pharmacological properties of this class of splice modulator.

Epoxide 2 Displays Potent Activity in Primary CLL-B Cells in Contrast to Its Precursor Alkene 19. We then screened the activity of **19** and **2** in primary CLL-B cells obtained from two CLL patients that displayed potent in vitro cytotoxic response (Figure 1), measured in the form of specific induced apoptosis (% SI), to **1a** (IC_{50} value of 54.1 ± 7.5 nM) and **1b** (IC_{50} value of 84.4 ± 1.2 nM). Interestingly, these studies indicated that alkene **19** did not display any activity (IC_{50} value >50 μM in both sets of cells). Epoxide **2**, however, was active (IC_{50} value of 153.0 ± 11.8 nM) with ∼3-fold loss of activity when compared to FD-895 (**1a**).

Compound 2 Modulates Splicing. We then turned to RT-PCR analysis to determine if the activity of **2** also included a splice response comparable to **1a** and **1b** in CLL-B cells. Using unspliced *RNU6A* and unmodulated *GAPDH* (top, Figure 5) as controls, we were able to obtain complementary splice modulation in all six genes selected from our prior studies to provide a diversity of intron retention (IR) response.[15a] This included comparable modification of IR in *DNAJB1*, *ARF4*, *PRPF4*, *RIOK3*, *SF3A1*, and *U2AF2* (Figure 4 and S2) from primary CLL-B cells. In contrast, alkene precursor **19** was inactive for all six genes (Figure 5), indicating that the epoxide in **2** is essential for activity.

Additionally, we were able to confirm that compound **2** also induced alternate splicing (AS) events. As shown in Figure 6,

DOI: 10.1021/jacs.5b13427
J. Am. Chem. Soc. 2016, 138, 5063−5068

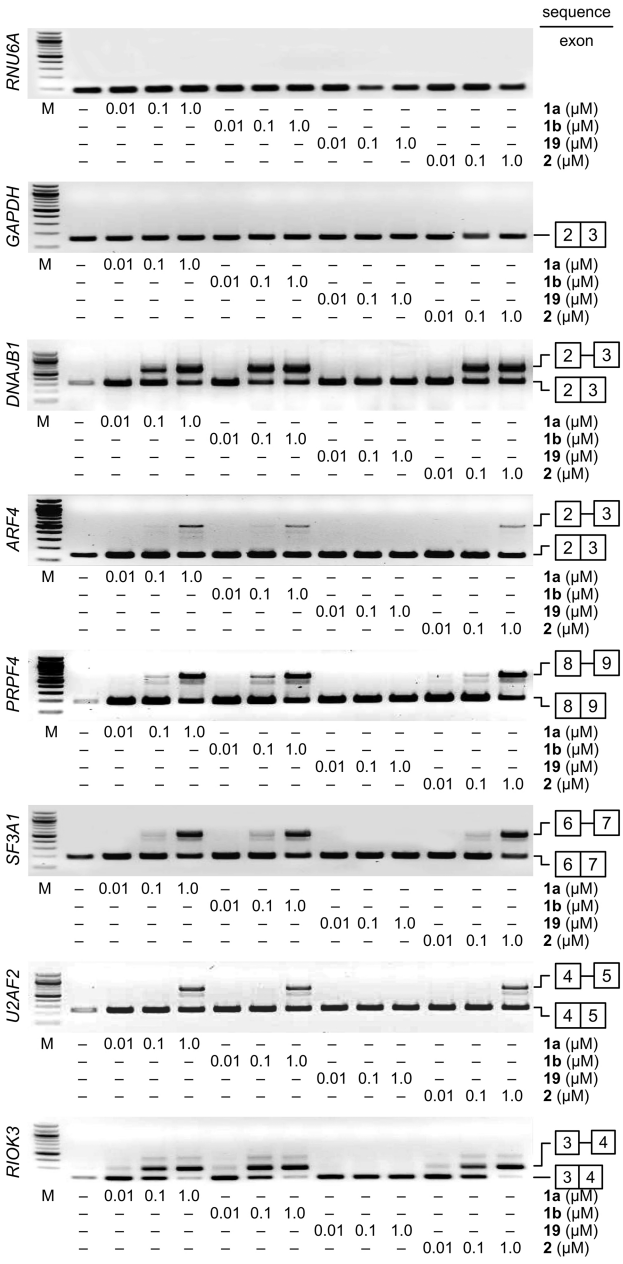

Figure 5. Compound **2** induces splice modulation via intron retention (IR) comparable to FD-895 (**1a**) and pladienolide B (**1b**) in CLL-B cells. The alkene precursor **19**, which was shown inactive in screening assays, did not induce IR. Genes *GAPDH* and *RNU6A* were used as unspliced and loading controls, respectively. Complementary qRT-PCR data has been provided in Figure S2.

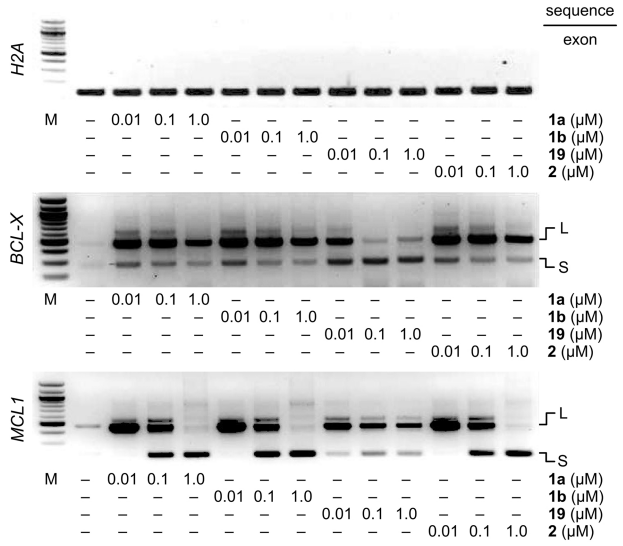

Figure 6. Compound **2** modulates alternate splicing (AS) in CLL-B cells, which is comparable to FD-895 (**1a**) and pladienolide B (**1b**). The alkene precursor **19**, which was shown inactive in screening assays, did not induce AS. *H2A* gene was used as unspliced loading control as depicted. S and L denote short and long isoforms, respectively.

treatment of CLL-B cells with **1a**, **1b**, and **2** resulted in a decrease in the long (anti-apoptotic) form and increased the expression of short (pro-apoptotic) form of *MCL1*. Similarly, *BCL-X* demonstrates comparable AS events (Figure 6). This indicates that cell death induced by **1a**, **1b**, and **2** is not exclusively derived through AS of *MCL1* but may also include other players. This fact is further supported by RNAseq analyses,[15a] which implicates the involvement of other pathways. Efforts are now underway to explore the roles of IR and AS events as well as to identify structural motifs that enrich specific events.

CONCLUSIONS

We now describe the preparation of a carbohydrate-derived spliceosome inhibitor **2** in a total of 22 steps, with the 12 longest linear steps from common building blocks (auxiliary **11**, D-glucose and propionaldehyde). Although complete in vitro and in vivo pharmacological analyses are underway, this analog's improved solubility, along with improved solubility in aqueous buffers, suggests an important advance in optimization of splice modulators.

Overall, this development offers several medicinal chemical benefits. First, it demonstrates that the pyran or macrolide core commonly associated with the known spliceosome inhibitors can be replaced with materials directly available from monosaccharides in the chiral pool. Second, it provides a means to prepare highly stable materials that lack rapid degradation and/or metabolic instability. Third, the use of a carbohydrate motif offers ready access to explore the SAR contained within the core unit (macrolide of **1a** and **1b** or pyran in **1c**, Figure 1). Here, one can envision application of the described route to provide derivatives with expanded functionality at the anomeric C1 center and stereoisomers at C1−C4 positions and to explore the use of deoxygenated materials and alternative ethers at C1−C4. Although to date there has been no structural information on the complex of any established splice modulator with the Sf3b component of the spliceosome, the subsequent integration of a rational design could deliver a carbohydrate-derived splice modulator with enhanced binding and reduced pharmacological risk.

ASSOCIATED CONTENT

Supporting Information

The Supporting Information is available free of charge on the ACS Publications website at DOI: 10.1021/jacs.5b13427.

Experimental procedures, characterization data for all new compounds, and full acknowledgments. (PDF)

DOI: 10.1021/jacs.5b13427
J. Am. Chem. Soc. 2016, 138, 5063−5068

AUTHOR INFORMATION

Corresponding Authors

*jlaclair@ucsd.edu

*mburkart@ucsd.edu

Notes

The authors declare no competing financial interest.

ACKNOWLEDGMENTS

This work was support by financial support from the Lymphoma Research Foundation (#285871), the NIH (PO1-CA081534), the University of California−San Diego Foundation Blood Cancer Research Fund and the Bennett Family Foundation. B. L. was supported by the NIH IRACDA K12 (GM068524) award. We thank Dr. Yongxuan Su for mass spectral analyses and Drs. Anthony Mrse and Xuemei Huang for assistance with acquiring NMR spectral data. We thank Prof. Thomas J. Kipps for providing the CLL patient-derived cells.

REFERENCES

(1) (a) Kotake, Y.; Sagane, K.; Owa, T.; Mimori-Kiyosue, Y.; Shimizu, H.; Uesugi, M.; Ishihama, Y.; Iwata, M.; Mizui, Y. *Nat. Chem. Biol.* **2007**, *3*, 570. (b) Kaida, D.; Motoyoshi, H.; Tashiro, E.; Nojima, T.; Hagiwara, M.; Ishigami, K.; Watanabe, H.; Kitahara, T.; Yoshida, T.; Nakajima, H.; Tani, T.; Horinouchi, S.; Yoshida, M. *Nat. Chem. Biol.* **2007**, *3*, 576. (c) Hasegawa, M.; Miura, T.; Kuzuya, K.; Inoue, A.; Won Ki, S.; Horinouchi, S.; Yoshida, T.; Kunoh, T.; Koseki, K.; Mino, K.; Sasaki, R.; Yoshida, M.; Mizukami, T. *ACS Chem. Biol.* **2011**, *6*, 229. (d) Bonnal, S.; Vigevani, L.; Valcarcel, J. *Nat. Rev. Drug Discovery* **2012**, *11*, 847.

(2) Seki-Asano, M.; Okazaki, T.; Yamagishi, M.; Sakai, N.; Takayama, Y.; Hanada, K.; Morimoro, S.; Takatsuki, A.; Mizoue, K. *J. Antibiot.* **1994**, *47*, 1395.

(3) (a) Mizui, Y.; Sakai, T.; Iwata, M.; Uenaka, T.; Okamoto, K.; Shimizu, H.; Yamori, T.; Yoshimatsu, K.; Asada, M. *J. Antibiot.* **2004**, *57*, 188. (b) Asai, N.; Kotake, Y.; Niijima, J.; Fukuda, Y.; Uehara, T.; Sakai, T. *J. Antibiot.* **2007**, *60*, 364.

(4) Salient examples of this family also include spliceostatin A, FR901465, meayamycin, and herboxidiene (GEX1A, **1c**), as described within the following: (a) Miller-Wideman, M.; Makkar, N.; Tran, M.; Isaac, B.; Biest, N.; Stonard, R. *J. Antibiot.* **1992**, *45*, 914. (b) Sakai, Y.; Yoshida, T.; Ochiai, K.; Uosaki, Y.; Saitoh, Y.; Tanaka, F.; Akiyama, T.; Akinaga, S.; Mizukami, T. *J. Antibiot.* **2002**, *55*, 855. (c) Liu, X.; Biswas, S.; Berg, M. G.; Antapli, C. M.; Xie, F.; Wang, Q.; Tang, M. C.; Tang, G. L.; Zhang, L.; Dreyfuss, G.; Cheng, Y. Q. *J. Nat. Prod.* **2013**, *76*, 685. (d) Nakajima, H.; Sato, B.; Fujita, T.; Takase, S.; Terano, H.; Okuhara, M. *J. Antibiot.* **1996**, *49*, 1196−203. (e) Meng, F.; McGrath, K. P.; Hoveyda, A. H. *Nature* **2014**, *513*, 367.

(5) For reports on the clinical trials on E7101, consult (a) Hong, D. S.; Kurzrock, R.; Naing, A.; Wheler, J. J.; Falchook, G. S.; Schiffman, J. S.; Faulkner, N.; Pilat, M. J.; O'Brien, J.; LoRusso, P. *Invest. New Drugs* **2014**, *32*, 436. (b) Dehm, S. M. *Clin. Cancer Res.* **2013**, *19*, 6064.

(6) (a) Villa, R.; Kashyap, M. K.; Kumar, D.; Kipps, T. J.; Castro, J. E.; La Clair, J. J.; Burkart, M. D. *J. Med. Chem.* **2013**, *56*, 6576. (b) Lagisetti, C.; Palacios, G.; Goronga, T.; Freeman, B.; Caufield, W.; Webb, T. R. *J. Med. Chem.* **2013**, *56*, 10033. (c) Albert, B. J.; Sivaramakrishnan, A.; Naka, T.; Czaicki, N. L.; Koide, K. *J. Am. Chem. Soc.* **2007**, *129*, 2648.

(7) Lagisetti, C.; Pourpak, A.; Jiang, Q.; Cui, X.; Goronga, T.; Morris, S. W.; Webb, T. R. *J. Med. Chem.* **2008**, *51*, 6220.

(8) (a) Convertini, P.; Shen, M.; Potter, P. M.; Palacios, G.; Lagisetti, C.; de la Grange, P.; Horbinski, C.; Fondufe-Mittendorf, Y. N.; Webb, T. R.; Stamm, S. *Nucleic Acids Res.* **2014**, *42*, 4947. (b) Webb, T. R.; Joyner, A. S.; Potter, P. M. *Drug Discovery Today* **2013**, *18*, 43. (c) Fan, L.; Lagisetti, C.; Edwards, C. C.; Webb, T. R.; Potter, P. M. *ACS Chem. Biol.* **2011**, *6*, 582−9. (d) Lagisetti, C.; Palacios, G.; Goronga, T.; Freeman, B.; Caufield, W.; Webb, T. R. *J. Med. Chem.* **2013**, *56*, 10033.

(9) Lagisetti, C.; Yermolina, M. V.; Sharma, L. K.; Palacios, G.; Prigaro, B. J.; Webb, T. R. *ACS Chem. Biol.* **2014**, *9*, 643.

(10) Kanada, R. M.; Itoh, D.; Nagai, M.; Niijima, J.; Asai, N.; Mizui, Y.; Abe, S.; Kotake, Y. *Angew. Chem., Int. Ed.* **2007**, *46*, 4350.

(11) Arai, K.; Buonamici, S.; Chan, B.; Corson, L.; Endo, A.; Gerard, B.; Hao, M. H.; Karr, C.; Kira, K.; Lee, L.; Liu, X.; Lowe, J. T.; Luo, T.; Marcaurelle, L. A.; Mizui, Y.; Nevalainen, M.; O'Shea, M. W.; Park, E. S.; Perino, S. A.; Prajapati, S.; Shan, M.; Smith, P. G.; Tivitmahaisoon, P.; Wang, J. Y.; Warmuth, M.; Wu, K. M.; Yu, L.; Zhang, H.; Zheng, G. Z.; Keaney, G. F. *Org. Lett.* **2014**, *16*, 5560.

(12) (a) He, H.; Ratnayake, A. S.; Janso, J. E.; He, M.; Yang, H. Y.; Loganzo, F.; Shor, B.; O'Donnell, C. J.; Koehn, F. E. *J. Nat. Prod.* **2014**, *77*, 1864−70. (b) Eustáquio, A. S.; Janso, J. E.; Ratnayake, A. S.; O'Donnell, C. J.; Koehn, F. E. *Proc. Natl. Acad. Sci. U. S. A.* **2014**, *111*, E3376.

(13) (a) Ghosh, A. K.; Veitschegger, A. M.; Sheri, V. R.; Effenberger, K. A.; Prichard, B. E.; Jurica, M. S. *Org. Lett.* **2014**, *16*, 6200. (b) Ghosh, A. K.; Chen, Z. H.; Effenberger, K. A.; Jurica, M. S. *J. Org. Chem.* **2014**, *79*, 5697. (c) Ghosh, A. K.; Ma, N.; Effenberger, K. A.; Jurica, M. S. *Org. Lett.* **2014**, *16*, 3154−7. (d) Effenberger, K. A.; Anderson, D. D.; Bray, W. M.; Prichard, B. E.; Ma, N.; Adams, M. S.; Ghosh, A. K.; Jurica, M. S. *J. Biol. Chem.* **2014**, *289*, 1938.

(14) (a) Larrayoz, M.; Blakemore, S. J.; Dobson, R. C.; Blunt, M. D.; Rose-Zerilli, M. J.; Walewska, R.; Duncombe, A.; Oscier, D.; Koide, K.; Forconi, F.; Packham, G.; Yoshida, M.; Cragg, M. S.; Strefford, J. C.; Steele, A. J. *Leukemia* **2016**, *30*, 351. (b) Schreiber, C. A.; Sakuma, T.; Izumiya, Y.; Holditch, S. J.; Hickey, R. D.; Bressin, R. K.; Basu, U.; Koide, K.; Asokan, A.; Ikeda, Y. *PLoS Pathog.* **2015**, *11*, e1005082. (c) Gao, Y.; Trivedi, S.; Ferris, R. L.; Koide, K. *Sci. Rep.* **2014**, *4*, 6098. (d) Gao, Y.; Koide, K. *ACS Chem. Biol.* **2013**, *8*, 895. (e) Gao, Y.; Vogt, A.; Forsyth, C. J.; Koide, K. *ChemBioChem* **2013**, *14*, 49. (f) Visconte, V.; Rogers, H. J.; Singh, J.; Barnard, J.; Bupathi, M.; Traina, F.; McMahon, J.; Makishima, H.; Szpurka, H.; Jankowska, A.; Jerez, A.; Sekeres, M. A.; Sauntharajah, Y.; Advani, A.S.; Copelan, E.; Koseki, H.; Isono, K.; Padgett, R. A.; Osman, S.; Koide, K.; O'Keefe, C.; Maciejewski, J. P.; Tiu, R. V. *Blood* **2012**, *120*, 3173. (g) Osman, S.; Albert, B. J.; Wang, Y.; Li, M.; Czaicki, N. L.; Koide, K. *Chem. - Eur. J.* **2011**, *17*, 895. (h) Albert, B. J.; McPherson, P. A.; O'Brien, K.; Czaicki, N. L.; Destefino, V.; Osman, S.; Li, M.; Day, B. W.; Grabowski, P. J.; Moore, M. J.; Vogt, A.; Koide, K. *Mol. Cancer Ther.* **2009**, *8*, 2308.

(15) (a) Kashyap, M. K.; Kumar, D.; Villa, R.; La Clair, J. J.; Benner, C.; Sasik, R.; Jones, H.; Ghia, E. M.; Rassenti, L. Z.; Kipps, T. J.; Burkart, M. D.; Castro, J. E. *Haematologica.* **2015**, *100*, 945. (b) Villa, R.; Mandel, A. L.; Jones, B. D.; La Clair, J. J.; Burkart, M. D. *Org. Lett.* **2012**, *14*, 5396.

(16) (a) Ernst, B.; Magnani, J. L. *Nat. Rev. Drug Discovery* **2009**, *8*, 661. (b) Jensen, K. J.; Brask, J. *Biopolymers* **2005**, *80*, 747. (c) Schweizer, F. *Angew. Chem., Int. Ed.* **2002**, *41*, 230.

(17) Structures were generated by positioning the atoms within the molecule using the known NOE correlations and minimizing with MM2 energy minimization. Efforts are now underway to complete a detailed solution structure of **1a**, **1b**, and **2**.

(18) Yan, C.; Hang, J.; Wan, R.; Huang, M.; Wong, C. C.; Shi, Y. *Science* **2015**, *349*, 1182.

(19) (a) Noel, A.; Delpech, B.; Crich, D. *Org. Lett.* **2012**, *14*, 4138. (b) Collins, D. J.; Hibberd, A. I.; Skelton, B. W.; White, A. H. *Aust. J. Chem.* **1998**, *51*, 681. (c) Pinilla, I. M.; Martínez, M. B.; Galbis, J. A. *Carbohydr. Res.* **2003**, *338*, 549. (c) Matwiejuk, M.; Thiem, J. *Chem. Commun.* **2011**, *47*, 8379.

(20) For instance, the first clinical lead, E-7101, bears a carbamate in place of the C29-C30 acetate; see Eskens, F. A.; Ramos, F. J.; Burger, H.; O'Brien, J. P.; Piera, A.; de Jonge, M. J.; Mizui, Y.; Wiemer, E. A.; Carreras, M. J.; Baselga, J.; Tabernero, J. *Clin. Cancer Res.* **2013**, *19*, 6296.

(21) (a) Nunes, C. D.; Vaz, P. D.; Félix, V.; Veiros, L. F.; Moniz, T.; Rangel, M.; Realista, S.; Mourato, A. C.; Calhorda, M. J. *Dalton Trans.* **2015**, *44*, 5125. (b) Rodríguez-Berríos, R. R.; Torres, G.; Prieto, J. A. *Tetrahedron* **2011**, *67*, 830.

(22) Dalisay, D. S.; Molinski, T. F. *J. Nat. Prod.* **2009**, *72*, 739.

DOI: 10.1021/jacs.5b13427
J. Am. Chem. Soc. 2016, 138, 5063−5068